© 2016. Published by The Company of Biologists Ltd | Journal of Experimental Biology (2016) 219, 3100-3105 doi:10.1242/jeb.137554

RESEARCH ARTICLE

Flowing water affects fish fast-starts: escape performance of the Hawaiian stream goby, *Sicyopterus stimpsoni*

Kelly M. Diamond[1,*], Heiko L. Schoenfuss[2], Jeffrey A. Walker[3] and Richard W. Blob[1]

ABSTRACT

Experimental measurements of escape performance in fishes have typically been conducted in still water; however, many fishes inhabit environments with flow that could impact escape behavior. We examined the influences of flow and predator attack direction on the escape behavior of fish, using juveniles of the amphidromous Hawaiian goby *Sicyopterus stimpsoni*. In nature, these fish must escape ambush predation while moving through streams with high-velocity flow. We measured the escape performance of juvenile gobies while exposing them to a range of water velocities encountered in natural streams and stimulating fish from three different directions. Frequency of response across treatments indicated strong effects of flow conditions and attack direction. Juvenile *S. stimpsoni* had uniformly high response rates for attacks from a caudal direction (opposite flow); however, response rates for attacks from a cranial direction (matching flow) decreased dramatically as flow speed increased. Mechanical stimuli produced by predators attacking in the same direction as flow might be masked by the flow environment, impairing the ability of prey to detect attacks. Thus, the likelihood of successful escape performance in fishes can depend critically on environmental context.

KEY WORDS: Biomechanics, Locomotion, Hydrodynamics, Fineness ratio, Acceleration, Predator–prey interactions

INTRODUCTION

The ability of prey to detect and respond to stimuli produced by predators is a critical factor in determining the outcome of predator–prey interactions. In fishes, one of the most common responses to predatory stimuli is the fast-start escape (Domenici, 2002; Hale, 1999; Webb, 1976), in which the body bends into a C- or an S-shape before unfolding to generate thrust to escape from the stimulus (Anderson, 1988). Fast-starts can be triggered by various stimuli, including visual sensory input (Eaton et al., 1977; Hale, 2002) and mechanical stimulation of the lateral line system (Stewart et al., 2013, 2014). Many aspects of fish biology can affect fast-start performance, including morphology (Law and Blake, 1996; Webb, 1976), developmental stage (Hale, 1996, 1999), behavior (Bohórquez-Herrera et al., 2013; Eaton et al., 1977) and physiology (Abrahams et al., 2007; Fu et al., 2015; Hale, 2002).

Although previous studies have clarified several intrinsic features of prey fish that can affect escape success, nearly all have tested fish in still water. Given the large number of aquatic habitats in which flowing water prevails, the potential impact of a major environmental variable on escape performance remains largely untested. One exception is work by D. G. Roche (Effects of biotic and physical stressors on fish swimming performance and behavior, PhD thesis, Australian National University, 2014), who demonstrated that unsteady flows produced by oceanic waves affect escape response latency and total distance traveled in juvenile reef fishes. Many other habitats (e.g. streams, rivers) exhibit predominantly unidirectional flows that could have different impacts on escape performance. Such conditions can be tractably simulated in lab settings using flow tanks (Lacey et al., 2012), but the impact of unidirectional flow on fish escapes has also received limited attention. Jayne and Lauder (1993) found differences in lateral displacement between escapes of bluegill sunfish in flowing versus still water, but did not compare many other aspects of performance. More recently, Chicoli and colleagues (2014) used flow tanks to compare escape responses from visual stimuli in schools of giant danio (*Devario aequipinnatus*). However, these trials were not designed to evaluate individual performance, or to stimulate the lateral line system, which is the primary source of sensory input for detecting and responding to aquatic predators in fish that employ fast-start escapes (Stewart et al., 2014). Finally, a recent study of bluegill escapes from acoustic-pressure wave stimuli found that escapes made while swimming in flow were less variable, but had lower velocities and accelerations, than escapes made in still water, and that performance was greater for escapes directed downstream versus those directed upstream (Anwar et al., 2016).

The probability of initiating an escape response varies with stimulus form (Domenici, 2002; Stewart et al., 2013, 2014) and the environment in which fish are attacked (Domenici, 2010a; Feitl et al., 2010). If flow masks the perception of predator-induced stimuli by the lateral line system, this could increase the percentage of fish that fail to perform an escape response. Fewer fish would be predicted to respond at higher flow speeds, particularly when attacked from the same direction as flow.

For fish that do detect and respond to stimuli, the fast-start escape behavior was, historically, viewed as a fixed-action pattern (Anderson, 1988; Domenici and Blake, 1991). Although some aspects of fast-start performance in fishes have been found to be independent of certain external factors (Binning et al., 2014; Fu et al., 2015), other fast-start variables have shown context dependency (Domenici, 2010a), and recent studies have indicated that viewing fast-starts as fixed actions is too simple (Abrahams et al., 2007; Domenici, 2010b; Marras et al., 2011; Tytell and Lauder, 2008). Studies of the black goby showed that fish react proportionally to the perceived strength of a stimulus (Turesson et al., 2009). If higher flow speeds dampen the ability of an individual to detect a stimulus, then larger escape angles might be expected in still water compared with flowing water. Alternatively, escapes might still be executed simply in a direction opposite to the

[1]Department of Biological Sciences, Clemson University, Clemson, SC 29634, USA. [2]Aquatic Toxicology Laboratory, Saint Cloud State University, Saint Cloud, MN 56301, USA. [3]Department of Biological Sciences, University of Southern Maine, Portland, ME 04103, USA.

*Author for correspondence (kmdiamo@clemson.edu)

K.M.D., 0000-0001-8639-6795

Received 14 January 2016; Accepted 22 July 2016

Journal of Experimental Biology

Journal of Experimental Biology (2016) 219, 3100-3105 doi:10.1242/jeb.137554

stimulus (Domenici and Blake, 1997), regardless of flow. It is also possible that flow could affect escape velocity and acceleration, depending on the direction of attack in relation to ambient flow. For example, if a fish were oriented upstream and attacked cranially (i.e. the same direction as stream flow), an escape oriented in the same direction as flow could increase the velocity and acceleration of the escape. Such impacts on fast-start performance could become more pronounced as flow speed increased.

Another factor that may influence escape performance under variable flow conditions is fish shape. Many fish exhibit a morphological trade-off, in which tall-bodied fish are better at escaping predation, but more streamlined fish experience lower drag (Blob et al., 2010; Domenici et al., 2008; Webb, 1984). Such morphological variation might correlate with how fishes execute escapes in flow. For example, when escaping in flowing water, fish with a more streamlined morphology might be expected to escape upstream (into oncoming flow) more often than those that are less streamlined.

To test for potential impacts of flow on escape behavior in fishes, we collected fast-start performance data from fish in which escape responses in flow have particular ecological relevance: juveniles of the amphidromous Hawaiian goby, *Sicyopterus stimpsoni*. Juvenile *S. stimpsoni* migrate upstream and against flow from larval habitats in the ocean to adult inland habitats in streams and rivers (Blob et al., 2010; Leonard et al., 2012; Moody et al., 2015). These gobies are well known for their ability to climb waterfalls (Fitzsimons et al., 1997; Schoenfuss and Blob, 2003); however, before reaching these predator-free environments, juvenile *S. stimpsoni* must navigate lower stream reaches with high densities of an ambush predator, the Hawaiian sleeper *Eleotris sandwicensis* (Blob et al., 2010; Maie et al., 2014).

To conduct our tests, we collected high-speed video of fast-start escapes by juvenile *S. stimpsoni* in response to multiple stimulus directions and across a gradient of flow speeds. With these data, we tested the following predictions: (1) the proportion of fish responding to stimuli will decrease if fish are attacked in the same direction as ambient flow, especially as flow speeds increase; (2) larger escape angles will occur in still water than in flow, or alternatively (3) escape angle is correlated with attack stimulus angle, regardless of flow speed; (4) more streamlined fish will escape upstream more frequently; and (5) fish attacked from the cranial direction will have higher peak velocities and accelerations than fish attacked from lateral or caudal directions as a result of aid from ambient flow, particularly as flow speed increases. Results from these analyses provide a new perspective on how the environment can influence escape performance of fishes in habitats commonly encountered in nature.

MATERIALS AND METHODS

Fish collection

Juvenile *Sicyopterus stimpsoni* (T. N. Gill 1860) (N=208; mean standard length, excluding caudal fin, 26.5±3.2 mm) were collected in March 2014 and March 2015 from Hakalau Stream (Island of Hawai'i). Fish were caught with dip nets in the stream estuary and transported, in stream water, to the Hilo field station of the Hawai'i Division of Aquatic Resources. Fish were housed in aerated stream water, and all trials were conducted between 24 and 48 h after capture.

All collection and animal use procedures were reviewed and approved by Clemson University (protocols 2011-057, 2015-009) and St Cloud State University (protocol 8-35) IACUCs. Specimens were collected with coordination by the Hawaii Division of Aquatic Resources (DAR), and under Special Activities Permit 2015-60.

Escape behavior trials and morphological data collection

Trials were conducted in a custom-built flow tank with continuous speed control and a 127.0×10.2×12.7 cm working area, fitted with a flow-through experimental chamber that restricted the filming area (22.9×10.2×12.7 cm) without the risk of fish encountering walls. Trials were filmed with a high-speed video camera (Fastec Highspec 2G, 1000 Hz), using a mirror angled at 45 deg to the clear bottom of the tank. *Sicyopterus stimpsoni* show strong positive orientation to current and commonly swim along benthic surfaces, periodically resting by attaching to substrates with a ventral sucker formed from their pelvic fins (Maie et al., 2012; Schoenfuss and Blob, 2003). Therefore, before applying a stimulus, all fish were allowed to come to a rest (i.e. stop moving) on the floor of the arena and orient in the same, head-upstream direction. No visible detachment motion was observed for recorded escape responses.

To stimulate escape responses, we modeled the mechanical (non-visual) stimulus imposed by predatory strikes by using a syringe connected to transparent tubing (4 mm diameter vinyl airline) to generate a rapid pulse of water directed towards the fish. We acknowledge that, in nature, fish could also use visual stimuli to detect predators. However, the primary predator of *S. stimpsoni* (*E. sandwicensis*) attacks from ambush (Maie et al., 2014), which likely limits the opportunity for visual perception, particularly for attacks from the side or rear; moreover, our initial applications of visual stimuli failed to elicit any escape responses, regardless of flow speed. To keep the application of the stimulus as consistent as possible across trials, the syringe was filled to the same volume (5 ml) and depressed by the operator with maximum force for each trial. Although rigid control of the distance between the stimulus and each fish was not possible, effort was made to maintain a consistent distance (~2 cm) across trials. Each trial was conducted on a new fish, with the water pulses directed parallel to the floor of the arena. To ensure maximal consistency of trial conditions within a block, the order of trial categories (see below) was not randomized, but rather each block of trials under a set of conditions was completed before conditions were changed. If the application of a stimulus failed to elicit an escape response from a fish, the trial was considered valid and contributed to evaluations of the proportion of fish that responded under each treatment; however, further performance variables were not calculated for these trials (i.e. average values of performance variables for treatments do not include zeros for trials with failed responses).

Trials were conducted at three flow speeds (still water, 15 cm s^{-1} and 30 cm s^{-1}), spanning a common range of flow speeds encountered by *S. stimpsoni* in nature (Fitzsimons et al., 1997). Flow tank speeds were calibrated with a flow meter (FlowMate 200, Marsh-McBirney Inc.). Water depth in the tank and the depth at which flow speed measurements were taken were consistent across all trials (12.7 and 2.5 cm, respectively). Attack stimuli were applied from one of three directions relative to the starting orientation of the fish (Fig. S1): cranial (0–60 deg; mean±circular s.d., 20.9±1.9 deg), lateral (61–120 deg, 89.9±1.9 deg) or caudal (121–180 deg, 164.5±2.5 deg). Thus, our study had nine treatment categories across all combinations of flow speed and stimulus direction. While attack angle was measured as a continuous variable, these angles were not evenly distributed, but clustered into three attack directions (Fig. S1), as intended by design. While we acknowledge that, within a single category, angles are not normally clustered around the mean of that category (Fig. S1B–E), each category was non-overlapping and averages are separated by over 60 deg (Fig. S1A). Consequently, we reduced these data to three attack directions (cranial, lateral and caudal) to better detect general patterns of

Journal of Experimental Biology (2016) 219, 3100-3105 doi:10.1242/jeb.137554

escape behavior as they related to the interactions with environmental flow conditions, which was the overall goal of this study. When we ran our model selection with continuous attack angles, our analyses produced the same best models (those with an Akaike information criterion difference, ΔAIC, below 2.0) as the model selection with categorical attack direction (Table S1).

After escape response trials, fish were killed by placing them in 0.25 g l^{-1} tricaine methanesulfonate (MS-222) solution, photographed for morphological measurements (performed using ImageJ 2014, NIH, Bethesda, MD, USA), and fixed in formalin. Specimens were later transferred to 70% ethanol for preservation. Fineness ratio was calculated for each fish as standard length divided by maximum height (Webb and Weihs, 1986). This measurement of overall body shape was considered to reflect relative streamlining, and was compared with escape performance to test for correlations with morphology.

Data analysis

For each trial, we digitized the midline of the fish from the first frame commencing movement, through to the end of stage two of the escape response, using DLT Data Viewer (Hedrick, 2008). From these data, the angle of attack was calculated from the first video frame of each trial as the angle between two vectors: the first from the center of mass to the most rostral point of the fish, and the second from the center of mass to the stimulus point (Domenici and Blake, 1991; Stewart et al., 2013). Based on data from 10 representative fish, we estimated the center of mass as occurring at a point along the midline approximately 44% of body length from the tip of the snout (Webb, 1976). Angle of escape was calculated for each video frame as the difference between the orientation of the center of mass-to-rostrum vector for that frame, and the orientation of that vector in the first analyzed frame (i.e. the starting orientation of the fish). Comparisons of escape angle across trials were based on the value measured at 30 ms after the escape response commenced. This time increment was chosen because it is within the average time taken by predatory *E. sandwicensis* to perform successful strikes on juvenile goby prey (Maie et al., 2014). We also measured escape angle at the end of stage one of the escape response (Table S2A; Fig. S2) to facilitate comparisons with other studies of escape responses based on such values. Because comparative patterns of performance based on these conventions were similar across our treatments, we focused our interpretation of results on the patterns derived from measurements at 30 ms, based on their ecological relevance for *S. stimpsoni*. Complementary to instantaneous escape angle, we also measured the angle between the stimulus and the orientation of the fish at the end of stage one of the escape response to evaluate the direction the fish takes with respect to the stimulus.

For each frame of a digitized sequence, we used a cubic spline interpolating function to identify the stretched-straight center of mass as the point 44% along the length of the midline from the tip of the snout. We computed smoothed position, velocity and acceleration of these points using a quintic spline (Walker et al., 2005). We used cross-validation to find a global optimum smoothing parameter used for all sequences. To find this parameter, we digitized five trials five times each, generating five replicate center-of-mass paths for each trial. For each pair of replicates within a trial, we designated one replicate the training replicate and the other the test replicate. We then found the parameter that minimized the root mean squared error (RMSE) in predicting the test replicate from splines fitted to the training replicate. The optimal parameter for the trial was the median of the parameters that minimized the RMSE computed for all 20 pair-wise combinations of training–test replicates. The global smoothing parameter was the median of the five optimal parameters for each trial with replicated measures. All quintic splines were fitted using the pspline package in R (version 1.0-16, https://cran.r-project.org/web/packages/pspline/index.html).

Statistical analysis

We explored the effects of stimulus direction (SD), flow speed (FS) and fineness ratio (FR) on five response variables: the probability of an escape response, the escape angle, the final angle from the stimulus, and escape performance (peak velocity and peak acceleration of the escape). The full model includes two fixed effects (SD and FS), one covariate (FR), and all interactions. In order to estimate effect sizes, we pooled across terms (main effects and interaction effects) that add little information to the predictability of the response. We fitted all sub-models of the fully factorial model and ranked these by ΔAIC, the difference between the AIC of the sub-model and the minimum AIC among all models (Burnham et al., 2011). AIC is a comparative measure of model fit adjusted by the number of parameters in the model so that more complex models are not necessarily better. We estimated effect sizes using the terms in the minimum AIC model, but also comment on additional models with small ΔAIC. To guide our interpretation of the experimental results, we also computed adjusted R^2 values of each sub-model. To model the probability of an escape response, we used a generalized linear model with a logit link function, which transforms the predicted values from a linear model to a distribution that approximates the response variable. Individuals were scored as 'success' if they responded to the stimulus with an escape response or 'failure' otherwise. We used McFadden's adjusted R^2 for the logistic model.

RESULTS

Proportion of fish responding to stimulus

Overall, 77% of the fish responded to the stimulus. The minimum AIC model (adjusted R^2=0.25) included SD, FS and their interaction, but not FR (Table 1, Fig. 1; Table S3A). SD and FS had a large non-additive effect on the frequency of response that was largely confined to the fish attacked cranially (Fig. 1). When fish

Table 1. Best models (those with a ΔAIC below 2.0) for response frequency, escape angle, angle from stimulus, peak velocity and peak acceleration

Model	ΔAIC	Adjusted R^2	R^2
Response frequency			
FS+SD+FS:SD	0.0	0.168	0.253
FR+FS+SD+FS:SD	1.9	0.190	0.254
Escape angle			
SD	0.0	0.110	0.124
SD+FR	1.6	0.106	0.126
Angle from stimulus			
SD	0.0	0.665	0.668
SD+FR	1.8	0.663	0.668
Peak velocity			
SD+FR+SD:FR	0.0	0.026	0.062
FR	0.5	−0.006	0.002
FS	1.9	−0.009	0.006
Peak acceleration			
SD+FR+SD:FR	0.0	0.066	0.100
SD+FR	0.9	0.047	0.068
FS+SD+FR+SD:FR	1.7	0.067	0.115
FR	1.8	0.026	0.034

All combinations of the variables flow speed (FS), stimulus direction (SD) and the covariate fineness ratio (FR) as well as all interactions were considered. Interactions are represented by colons. For full model analysis results, see Tables S2B and S3A–D.

Journal of Experimental Biology

Journal of Experimental Biology (2016) 219, 3100-3105 doi:10.1242/jeb.137554

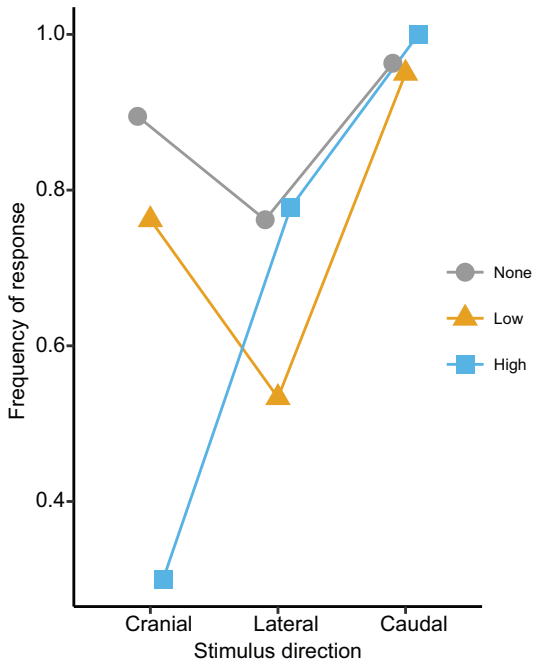

Fig. 1. Plot of the frequency of response by juvenile *Sicyopterus stimpsoni* for each stimulus direction: cranial, lateral and caudal. Flow speeds are represented by different symbols and coded 'none' for still water, 'low' for 15 cm s^{-1} flow and 'high' for 30 cm s^{-1} flow.

were attacked cranially, there was a dramatic increase in response failure as flow speed increased, moving from 11% failure in still water, to 24% failure at 15 cm s^{-1}, to 70% failure at 30 cm s^{-1} (Fig. 1). In contrast, for fish attacked caudally, the percentage of fish responding was consistently high (95% or higher) regardless of flow speed (Fig. 1). The second and third smallest AIC models included FR as an additive effect (ΔAIC=1.9) and a non-additive effect interacting with FS (ΔAIC=2.5). The non-adjusted R^2 for these models increased less than 1.7% with these additions (Table 1; Table S3A), indicating that FR has a very noisy and possibly inconsistent effect across SD by FS treatments.

Angular movements

The grand mean escape angle (relative to the starting orientation of the fish) was 43.7 deg and ranged from 30.0 to 69.8 deg among the FS by SD treatments (Table S4). The minimum AIC model included only SD (adjusted R^2=0.11; Table 1; Table S3B). This result is evident in Fig. 2A, which shows a large SD but not FS effect, with larger escape angles for fish stimulated from the front (cranial) regardless of FS. Ignoring FS and FR, fish attacked cranially increased escape angle by 26.5 deg (95% confidence interval, CI: 11.9–41.0 deg) and 26.9 deg (95% CI: 13.7–40.0 deg) relative to lateral and caudal attacks. If added to the minimum AIC model, FR has a negative, but seemingly trivial, effect on escape angle (β=−2.7 deg per unit fineness, 95% CI: −11.3 to 6.0 deg). When escape angle was measured relative to the stimulus, rather than the starting orientation of the fish, the minimum AIC model also included only SD (adjusted R^2=0.67; Table 1; Table S2B). This result is evident in Fig. 2B, which again shows a large SD but not FS effect, with escape angle from stimulus increasing as attack angle increases.

Peak velocity and acceleration

The mean peak escape velocity was 74.8±2.12 cm s^{-1} (mean±s.e.m.). No combination of SD, FS and FR explained more than 3% of the variance in peak escape velocity (Table S3C). Consequently, we do not report or interpret the measured effect sizes. The mean peak escape acceleration was 7976.3±268.0 cm s^{-2}. The minimum AIC model (adjusted R^2=0.07) included SD, FR and their interaction, but not FS (Table 1; Table S3D). Fig. 3 shows that peak escape acceleration increases with FR, but the magnitude depends on the SD. Ignoring FS (the minimum AIC model), the effect of FR was highest in the cranially stimulated fish (β: 26.5 cm s^{-2} per unit fineness, 95% CI: 9.2–43.9 cm s^{-2}), intermediate in the laterally stimulated fish (β: 8.4 cm s^{-2}, 95% CI: −14.9 to 31.6 cm s^{-2}), and lowest in the caudally stimulated fish (β: 3.6 cm s^{-2}, 95% CI: −17.4 to 24.6 cm s^{-2}). The consequence of the interaction is that at high (but not low) FR, SD has a large effect. For example, at FR equal to 9.5, cranially stimulated fish are expected to peak at 125.3 cm s^{-2} (95% CI: 97.4–153.2 cm s^{-2}), whereas laterally stimulated fish are expected to peak at 93.4 cm s^{-2} (95% CI: 73.6 –113.2 cm s^{-2}), and caudally stimulated fish are expected to peak at only 78.9 cm s^{-2} (95% CI: 62.5–95.2 cm s^{-2}).

DISCUSSION

Previous studies of how flow conditions affect the escape responses of fishes have been limited. Our experiments show that flowing water can have a range of effects on escape responses, though these effects may be complex and depend on the direction of attack.

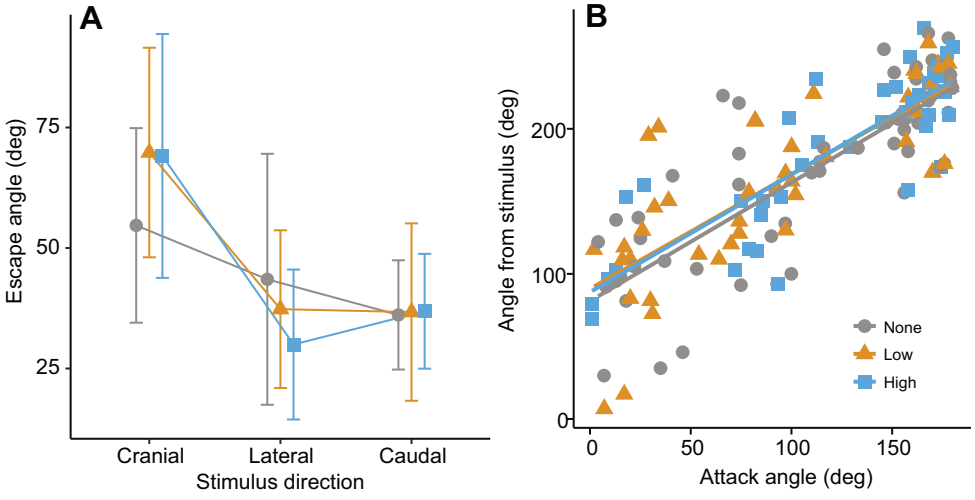

Fig. 2. Plots of angular movements by juvenile *S. stimpsoni* during escape responses. (A) Mean (±circular s.e.m.) escape angle for each stimulus direction (cranial, lateral or caudal), calculated 30 ms following the initiation of the fast-start escape response. (B) Scatterplot of the total angle from the stimulus to the position of the juvenile at the end of the first stage of the escape response for each attack. Attack angle is defined in relation to the original orientation of the fish. For both plots, flow speed is represented by different symbols and coded 'none' for still water, 'low' for 15 cm s^{-1} flow and 'high' for 30 cm s^{-1} flow.

Journal of Experimental Biology (2016) 219, 3100-3105 doi:10.1242/jeb.137554

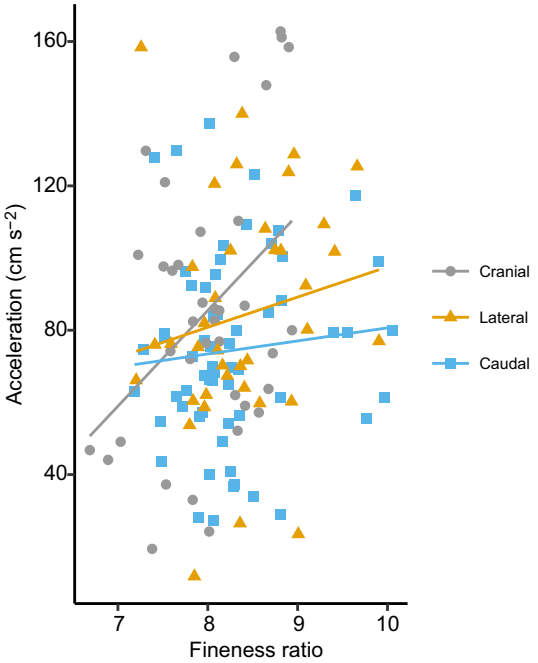

Fig. 3. Scatter plot diagram of peak acceleration plotted against fineness ratio (standard length/maximum height) for each fish that exhibited an escape response. Different symbols represent the three different stimulus directions: cranial, lateral and caudal. A line of best fit is plotted for each stimulus direction: cranial $y=26.52x+2651.83$, lateral $y=8.37x-1815.31$ and caudal $y=3.61x-2290.65$.

The strongest indication that flow conditions can affect the escape responses of fish emerged through comparisons of response failure across treatments. Whereas juvenile *S. stimpsoni* had uniformly high response rates for attacks from a caudal direction, response rates for attacks from the cranial direction decreased dramatically as flow speed increased, shifting from 11% failure in still water to 70% failure at 30 cm s^{-1} (Table S4; Fig. 1). The frequent failure of fish to respond to flow pulses from the cranial direction might be the result of high flows masking the stimulus, thereby reducing the ability of the prey's lateral line to detect the simulated predator. In contrast, proprioceptive capacity of the fins (e.g. caudal fin) may facilitate responses to flow pulses from the caudal direction that oppose ambient flow (Flammang and Lauder, 2013; Williams et al., 2013). The strength of a stimulus relative to the strength of alternative environmental cues has been shown to influence the type and number of escape responses in animals, including fish (Abrahams and Kattenfeld, 1997; Domenici, 2010a; D. G. Roche, Effects of biotic and physical stressors on fish swimming performance and behavior, PhD thesis, Australian National University, 2014). Moreover, fish with compromised lateral line systems typically fail to perform fast-start escapes in response to stimuli, even when the visual system remains intact (Stewart et al., 2014; but see Mirjany et al., 2011). Considering the frequent failure of juvenile *S. stimpsoni* to respond to cranial attacks in high flow, it is possible that positively rheotactic fish like this species may be most vulnerable to attacks from the cranial direction during upstream migrations. Field observations of attack directions by *E. sandwicensis* on migrating gobies could test whether these predators typically attack from directions or in flow environments that mask their approach (Rubin et al., 2016).

When they responded, juvenile *S. stimpsoni* attacked from a cranial direction showed greater escape angles than fish attacked from other directions, regardless of flow (Fig. 2A). We had initially predicted that still water trials would result in greater escape angles than trials in flow, potentially due to hydrodynamic drag imposed by flow that could impede movement by escaping fishes. Instead, at least during attacks from the cranial direction, it is possible that drift imposed by flow might increase escape angles of fish. This passive explanation would be consistent with behavioral evidence indicating that the underlying neural command of fast-starts is ballistic, and does not use additional sensory information from stimuli once movement begins (Eaton and Emberley, 1991). Such responses would, thus, override the strong directional rheotaxis exhibited by juvenile *S. stimpsoni* during upstream migrations (Leonard et al., 2012; Schoenfuss and Blob, 2003). Moreover, because all fish were oriented upstream at the start of trials, their initial rotation during an escape was in a direction toward the predator when they were attacked from a caudal direction. Such initial responses could be disadvantageous, even if modulated in later stages of the escape.

We found no patterns in the effects of stimulus direction or flow speed on peak escape velocity (Table S3C). Many studies have found limited responses of fast-start velocity to a variety of changing conditions (Feitl et al., 2010; Fu et al., 2015). Because the movement of water from the jet stimulus was not visible, it was not possible to evaluate response latency in this study, but further trials (e.g. with jets of dyed water) could be performed to test for such responses.

In contrast to peak velocity, peak acceleration showed stronger effects exerted by stimulus direction and fineness ratio. For attacks from the cranial direction at intermediate flow speeds, more streamlined fish exhibited higher peak accelerations than taller-bodied fish. These results support the potential for ambient flow conditions to affect fast-start escapes (Anwar et al., 2016). Specifically, when fish are oriented with the head into the flow, escapes from cranial attacks could be aided by ambient flow during movement away from a predator. Although these patterns were limited to a single treatment, they indicate potentially complicated relationships between body shape and fast-start performance (Walker, 1997; Webb, 1978).

Migratory fishes that depend on flow stimuli, such as *S. stimpsoni*, have been used to detect early changes in stream ecosystems in response to anthropogenic activities (Donaldson et al., 2013; Schoenfuss and Blob, 2007). Many streams can be subject to rapid changes in flow conditions (e.g. flash flooding), but little is known about how changes in flow conditions affect stream communities (Fitzsimons et al., 1997; Julius, 2007). The results of this study show that the likelihood of successful functional performance can depend critically on environmental context. Thus, understanding the escape performance of fish in flow environments can contribute to understanding how predator–prey interactions might be affected by the prospect of changing environmental conditions (Abrahams et al., 2007).

Acknowledgements

We thank M. Childress, M. Sears and W. Bridges for help with statistical analyses; K. Vest, T. Offerle and A. Rubin for contributing to video analysis; D. Ellerby for providing an advance copy of a manuscript under review; A. Ciccoli for discussion; Hilo DAR staff (L. Nishiura, T. Shimoda, T. Sakihara, T. Shindo and N. Ahu) for facility access, field assistance and hospitality; and R. Nishimoto, K. Peyton and C. Gewecke for coordinating field research permission.

Competing interests

The authors declare no competing or financial interests.

Author contributions

K.M.D., H.L.S. and R.W.B. designed the study and collected the data; K.M.D. and J.A.W. analyzed the data; all authors contributed to manuscript drafts and revisions.

Funding
Support was provided by Sigma Xi (K.M.D.), Clemson Creative Inquiry grant no. 479 (R.W.B.) and St Cloud State University SCSU-211228 Short-Term Faculty Improvement Grant (H.L.S.).

Data availability
Fish specimens from this study are curated in the Campbell Museum of Natural History at Clemson University. Data table and R sweave code for this project can be found at the following link: https://github.com/middleprofessor/Goby.

Supplementary information
Supplementary information available online at
http://jeb.biologists.org/lookup/doi/10.1242/jeb.137554.supplemental

References

Abrahams, M. V. and Kattenfeld, M. G. (1997). The role of turbidity as a constraint on predator-prey interactions in aquatic environments. *Behav. Ecol. Sociobiol.* **40**, 169-174.
Abrahams, M. V., Mangel, M. and Hedges, K. (2007). Predator-prey interactions and changing environments: who benefits? *Philos. Trans. R. Soc. B Biol. Sci.* **362**, 2095-2104.
Anderson, J. J. (1988). A neural model for visual activation of startle behavior in fish. *J. Theor. Biol.* **131**, 279-288.
Anwar, S. B., Cathcart, K., Darakananda, K., Gaing, A. N., Shin, S. Y., Vronay, X., Wright, D. N. and Ellerby, D. J. (2016). The effects of steady swimming on fish escape performance. *J. Comp. Phys. A* **202**, 425-433.
Binning, S. A., Barnes, J. I., Davies, J. N., Backwell, P. R. Y., Keogh, J. S. and Roche, D. G. (2014). Ectoparasites modify escape behaviour, but not performance, in a coral reef fish. *Anim. Behav.* **93**, 1-7.
Blob, R. W., Kawano, S. M., Moody, K. N., Bridges, W. C., Maie, T., Ptacek, M. B., Julius, M. L. and Schoenfuss, H. L. (2010). Morphological selection and the evaluation of potential tradeoffs between escape from predators and the climbing of waterfalls in the Hawaiian stream goby *Sicyopterus stimpsoni*. *Integr. Comp. Biol.* **50**, 1185-1199.
Bohórquez-Herrera, J., Kawano, S. M. and Domenici, P. (2013). Foraging behavior delays mechanically-stimulated escape responses in fish. *Integr. Comp. Biol.* **53**, 780-786.
Burnham, K. P., Anderson, D. R. and Huyvaert, K. P. (2011). AIC model selection and multimodel inference in behavioral ecology: some background, observations, and comparisons. *Behav. Ecol. Sociobiol.* **65**, 23-35.
Chicoli, A., Butail, S., Lun, Y., Bak-Coleman, J., Coombs, S. and Paley, D. A. (2014). The effects of flow on schooling *Devario aequipinnatus*: school structure, startle response and information transmission. *J. Fish Biol.* **84**, 1401-1421.
Domenici, P. (2002). The visually mediated escape response in fish: predicting prey responsiveness and the locomotor behaviour of predators and prey. *Mar. Freshwater Behav. Physiol.* **35**, 87-110.
Domenici, P. (2010a). Context-dependent variability in the components of fish escape response: integrating locomotor performance and behavior. *J. Exp. Zool. A Ecol. Genet. Physiol.* **313A**, 59-79.
Domenici, P. (2010b). Escape responses in fish: kinematics, performance and behavior. In *Fish Locomotion* (ed. P. Domenici and B. G. Kapoor), pp. 123-170. Enfield: Science Publishers.
Domenici, P. and Blake, R. W. (1991). The kinematics and performance of the escape response in angelfish (*Pterophyllum eimekei*). *J. Exp. Biol.* **156**, 187-205.
Domenici, P. and Blake, R. W. (1997). The kinematics and performance of fish fast-start swimming. *J. Exp. Biol.* **200**, 1165-1178.
Domenici, P., Turesson, H., Brodersen, J. and Brönmark, C. (2008). Predator-induced morphology enhances escape locomotion in crucian carp. *Proc. R. Soc. B Biol. Sci.* **275**, 195-201.
Donaldson, J. A., Ebner, B. C. and Fulton, C. J. (2013). Flow velocity underpins microhabitat selection by gobies of the Australian wet tropics. *Freshwater Biol.* **58**, 1038-1051.
Eaton, R. C. and Emberley, D. S. (1991). How stimulus direction determines the trajectory of the Mauthner-initiated escape response in a teleost fish. *J. Exp. Biol.* **161**, 469-487.
Eaton, R. C., Bombardieri, R. A. and Meyer, D. L. (1977). The Mauthner-initiated startle response in teleost fish. *J. Exp. Biol.* **66**, 65-81.
Feitl, K. E., Ngo, V. and McHenry, M. J. (2010). Are fish less responsive to a flow stimulus when swimming? *J. Exp. Biol.* **213**, 3131-3137.
Fitzsimons, J. M., Schoenfuss, H. L. and Schoenfuss, T. C. (1997). Significance of unimpeded flows in limiting the transmission of parasites from exotics to Hawaiian stream fishes. *Micronesica* **30**, 117-125.
Flammang, B. E. and Lauder, G. V. (2013). Pectoral fins aid in navigation of a complex environment by bluegill sunfish under sensory deprivation conditions. *J. Exp. Biol.* **216**, 3084-3089.
Fu, C., Fu, S.-J., Yuan, X.-Z. and Cao, Z.-D. (2015). Predator-driven intra-species variation in locomotion, metabolism and water velocity preference in pale chub (*Zacco platypus*) along a river. *J. Exp. Biol.* **218**, 255-264.
Hale, M. E. (1996). The development of fast-start performance in fishes: escape kinematics of the chinook salmon (*Oncorhynchus tshawytscha*). *Amer. Zool.* **36**, 695-709.
Hale, M. E. (1999). Locomotor mechanics during early life history: effects of size and ontogeny on fast-start performance of Salmonid fishes. *J. Exp. Biol.* **202**, 1465-1479.
Hale, M. E. (2002). S- and C-start escape responses of the muskellunge (*Esox masquinongy*) require alternative neuromotor mechanisms. *J. Exp. Biol.* **205**, 2005-2016.
Hedrick, T. L. (2008). Software techniques for two- and three-dimensional kinematic measurements of biological and biomimetic systems. *Bioinspir. Biomim.* **3**, 034001.
Jayne, B. C. and Lauder, G. V. (1993). Red and white muscle activity and kinematics of the escape response of the bluegill sunfish during swimming. *J. Comp. Physiol. A* **173**, 495-508.
Julius, M. L. (2007). Why sweat the small stuff: the importance of microalgae in Hawaiian stream ecosystems. *Bishop Mus. Bull. Cult. Environ. Stud.* **3**, 183-193.
Lacey, R. W. J., Neary, V. S., Liao, J. C., Enders, E. C. and Tritico, H. M. (2012). The IPOS framework: linking fish swimming performance in altered flows from laboratory experiments to rivers. *River Res. Appl.* **28**, 429-443.
Law, T. C. and Blake, R. W. (1996). Comparison of the fast-start performances of closely related, morphologically distinct threespine sticklebacks (*Gasterosteus* spp.). *J. Exp. Biol.* **199**, 2595-2604.
Leonard, G., Maie, T., Moody, K. N., Schrank, G. D., Blob, R. W. and Schoenfuss, H. L. (2012). Finding paradise: cues directing the migration of the waterfall climbing Hawaiian gobioid *Sicyopterus stimpsoni*. *J. Fish Biol.* **81**, 903-920.
Maie, T., Schoenfuss, H. L. and Blob, R. W. (2012). Performance and scaling of a novel locomotor structure: adhesive capacity of climbing gobiid fishes. *J. Exp. Biol.* **215**, 3925-3936.
Maie, T., Furtek, S., Schoenfuss, H. L. and Blob, R. W. (2014). Feeding performance of the Hawaiian sleeper, *Eleotris sandwicensis* (Gobioidei: Eleotridae): correlations between predatory functional modulation and selection pressures on prey. *Biol. J. Linnean Soc.* **111**, 359-374.
Marras, S., Killen, S. S., Claireaux, G., Domenici, P. and McKenzie, D. J. (2011). Behavioural and kinematic components of the fast-start escape response in fish: individual variation and temporal repeatability. *J. Exp. Biol.* **214**, 3102-3110.
Mirjany, M., Preuss, T. and Faber, D. S. (2011). Role of the lateral line mechanosensory system in directionality of goldfish auditory evoked escape response. *J. Exp. Biol.* **214**, 3358-3367.
Moody, K. N., Hunter, S. N., Childress, M. J., Blob, R. W., Schoenfuss, H. L., Blum, M. J. and Ptacek, M. B. (2015). Local adaptation despite high gene flow in the waterfall-climbing Hawaiian goby, *Sicyopterus stimpsoni*. *Mol. Ecol.* **24**, 545-563.
Rubin, A. M., Diamond, K. M., Schoenfuss, H. L. and Blob, R. W. (2016). Field observation of intraspecific and predatory attack behaviors of the Hawaiian sleeper fish, *Eleotris sandwicensis*. *Integr. Comp. Biol.* **56** Suppl. 1, e53.
Schoenfuss, H. L. and Blob, R. W. (2003). Kinematics of waterfall climbing in Hawaiian freshwater fishes (Gobiidae): vertical propulsion at the aquatic–terrestrial interface. *J. Zool.* **261**, 191-205.
Schoenfuss, H. L. and Blob, R. W. (2007). The importance of functional morphology for fishery conservation and management: applications to Hawaiian amphidromous fishes. *Bishop Mus. Bull. Cult. Environ. Stud.* **3**, 125-141.
Stewart, W. J., Cardenas, G. S. and McHenry, M. J. (2013). Zebrafish larvae evade predators by sensing water flow. *J. Exp. Biol.* **216**, 388-398.
Stewart, W. J., Nair, A., Jiang, H. and McHenry, M. J. (2014). Prey fish escape by sensing the bow wave of a predator. *J. Exp. Biol.* **217**, 4328-4336.
Turesson, H., Satta, A. and Domenici, P. (2009). Preparing for escape: anti-predator posture and fast-start performance in gobies. *J. Exp. Biol.* **212**, 2925-2933.
Tytell, E. D. and Lauder, G. V. (2008). Hydrodynamics of the escape response in bluegill sunfish, *Lepomis macrochirus*. *J. Exp. Biol.* **211**, 3359-3369.
Walker, J. A. (1997). Ecological morphology of lacustrine threespine stickleback *Gasterosteus aculeatus* L. (Gasterosteidae) body shape. *Biol. J. Linnean Soc.* **61**, 3-50.
Walker, J. A., Ghalambor, C. K., Griset, O. L., McKenney, D. and Reznick, D. N. (2005). Do faster starts increase the probability of evading predators? *Func. Ecol.* **19**, 808-815.
Webb, P. W. (1976). The effect of size on the fast-start performance of rainbow trout *Salmo gairdneri*, and a consideration of piscivorous predator-prey interactions. *J. Exp. Biol.* **65**, 157-178.
Webb, P. W. (1978). Fast-start performance and body form in seven species of teleost fish. *J. Exp. Biol.* **74**, 211-226.
Webb, P. W. (1984). Body form, locomotion and foraging in aquatic vertebrates. *Amer. Zool.* **24**, 107-120.
Webb, P. W. and Weihs, D. (1986). Functional locomotor morphology of early life history stages of fishes. *Trans. Am. Fish. Soc.* **115**, 115-127.
Williams, R., IV, Neubarth, N. and Hale, M. E. (2013). The function of fin rays as proprioceptive sensors in fish. *Nat. Commun.* **4**, 1729.

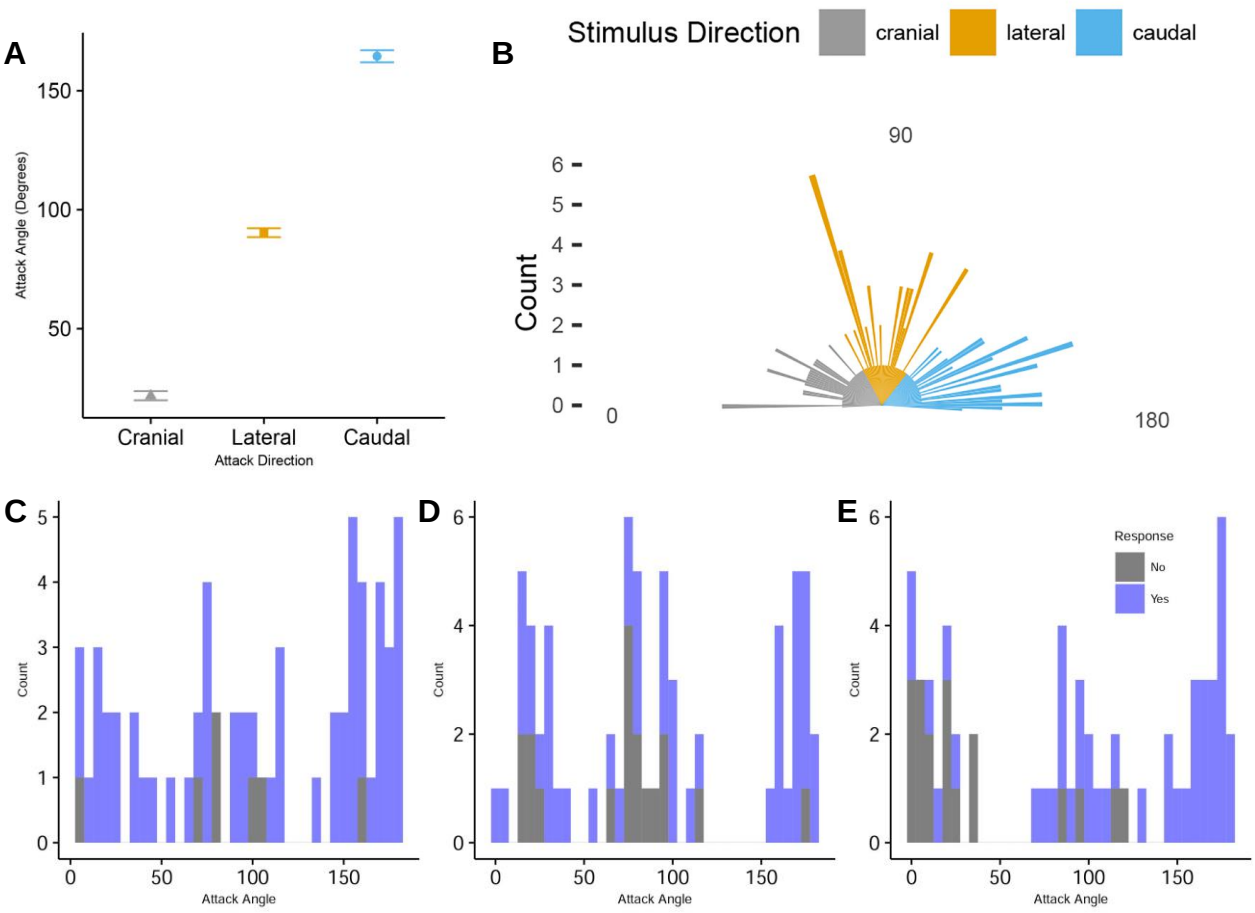

Fig. S1. Distribution of attack angles. Attack angles were calculated from the first video frame of each trial as the angle between two vectors, both originating at the fish center of mass and ending at the fish rostrum and stimulus point, respectively. 0° implies the stimulus was oriented directly at the rostrum of the fish, and 180° directly at the tail of the fish, at the commencement of the trial. Study design intended stimulus directions to be categorical, producing gaps in sampling between categories (minimum of 10°) rather than systematic, continuous sampling. Here we present three representations of the distribution of our attack angles. In (A) we plot the averages and circular standard deviations of attack angles when grouped by our three categorical attack directions: cranial (light grey), lateral (orange), and caudal (light blue). These groups are non-overlapping and their averages are separated by over 60°. (B) Circular plot of our attack angles. Line lengths represent the number of fish attacked at the given angle. (C, D, E) Stacked histograms of responses of individuals across all attack directions for our three flow speeds: still water (C), 15 cm sec^{-1} (D), and 30 cm sec^{-1} (E). Each bar represents the number of fish (in a five degree range) that either responded or did not respond when attacked. Because multiple fish responded differently at the same attack angle, the number of fish that did respond (dark blue) are stacked on top of the number of fish that did not respond (dark grey).

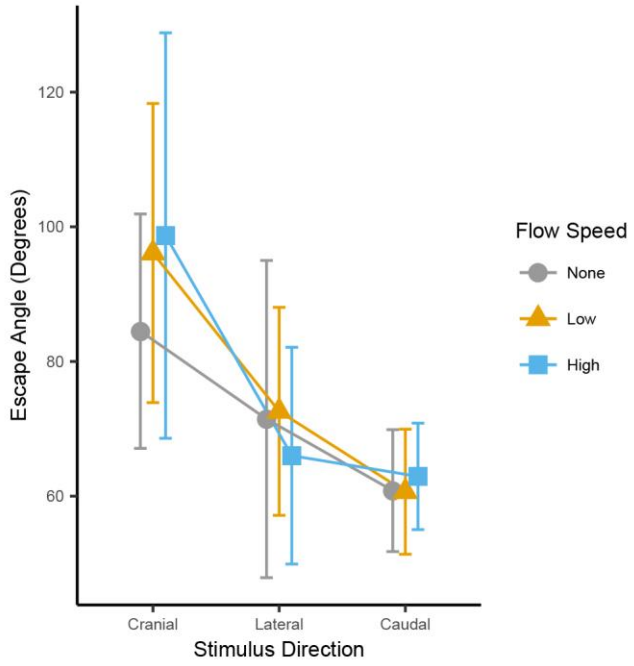

Fig. S2. Plot of the average escape angle for each stimulus direction, when escape angles are calculated for the end of stage 1 of the fast- start escape response. Flow speeds are represented by differently shaped points and coded "None" for still water (circles), "Low" for 15 cm sec^{-1} (triangles), and "High" for 30 cm sec^{-1} (squares). Whiskers for each point represent its standard error.

Table S1. Model selection for variables when attack angle was considered a continuous variable. (A) Best models (those with a ΔAIC below 2.0) and (B) Full model selection for fast-start response, escape angle, peak velocity, and peak acceleration. The best model for each variable below matches those of the analysis in which attack direction was analyzed as a categorical variable.

A Best Models

Model	ΔAIC	Adjusted R^2	R^2
Response			
FS + SD + FS:SD	0.0	0.122	0.183
Escape Angle			
SD + FR	0.0	0.090	0.104
SD	0.0	0.083	0.090
SD + FR + SD:FR	1.6	0.086	0.107
Peak Velocity			
SD + FR + SD:FR	0.0	0.042	0.065
Peak Acceleration			
SD + FR + SD:FR	0.0	0.101	0.122
SD + FS + FR + SD:FS + SD:FR	1.9	0.114	0.162

B Full models

Model	ΔAIC	Adjusted R^2	R^2
Response			
FS + SD + FS:SD	0.0	0.122	0.183
SD + FS + FR + SD:FS + SD:FR	2.0	0.112	0.193
FR + FS + SD + FS:SD	2.0	0.113	0.183
FS + SD + FR + FS:SD + FS:FR + SD:FR	2.6	0.109	0.210
FS + SD	2.6	0.109	0.150
FS + SD + FR + FS:SD + FS:FR	3.4	0.105	0.196
FS + SD + FR + FS:SD + FS:FR + SD:FR + FS:SD:FR	4.4	0.100	0.222
FS + SD + FR	4.6	0.099	0.150
SD	5.1	0.097	0.117
FS + SD + FR + SD:FR	5.8	0.093	0.154
SD + FS + FR + FS:FR	6.0	0.092	0.163
FR + FS + SD + FR:FS + FR:SD	6.5	0.089	0.170
SD + FR	7.1	0.087	0.117
SD + FR + SD:FR	8.4	0.080	0.121
FS	22.0	0.012	0.042
FS + FR + FS:FR	23.1	0.006	0.066
FS + FR	23.4	0.004	0.045
FR	27.9	-0.019	0.002
Escape Angle			
SD + FR	0.0	0.090	0.104
SD	0.0	0.083	0.090
SD + FR + SD:FR	1.6	0.086	0.107
SD + FS + FR + FS:FR	3.1	0.095	0.138
FS + SD + FR	3.6	0.078	0.107
FS + SD	3.7	0.070	0.092
FR + FS + SD + FR:FS + FR:SD	4.5	0.092	0.142
FS + SD + FR + SD:FR	5.1	0.074	0.110
FS + SD + FR + FS:SD + FS:FR	6.4	0.085	0.142
FR + FS + SD + FS:SD	7.0	0.068	0.112
FS + SD + FS:SD	7.0	0.061	0.097
FS + SD + FR + FS:SD + FS:FR + SD:FR	7.3	0.086	0.150
SD + FS + FR + SD:FS + SD:FR	7.9	0.068	0.119
FR	8.9	0.018	0.026
FS + SD + FR + FS:SD + FS:FR + SD:FR + FS:SD:FR	10.8	0.074	0.153
FS + FR	11.3	0.015	0.038
FS + FR + FS:FR	11.5	0.027	0.065
FS	12.8	-0.005	0.011

Peak Velocity			
SD + FR + SD:FR	0.0	0.042	0.065
FR + FS + SD + FR:FS + FR:SD	1.5	0.059	0.110
FS + SD + FR + SD:FR	2.7	0.037	0.074
FR	4.3	-0.005	0.003
FS + SD + FR + FS:SD + FS:FR + SD:FR	4.4	0.051	0.117
SD	4.5	-0.006	0.002
SD + FS + FR + SD:FS + SD:FR	5.5	0.030	0.082
FS	5.7	-0.008	0.007
SD + FR	6.1	-0.012	0.004
FS + FR + FS:FR	6.9	0.005	0.044
FS + FR	7.2	-0.012	0.011
FS + SD	7.6	-0.015	0.008
FS + SD + FR + FS:SD + FS:FR + SD:FR + FS:SD:FR	7.8	0.040	0.122
SD + FS + FR + FS:FR	8.8	-0.003	0.044
FS + SD + FR	9.1	-0.020	0.012
FS + SD + FS:SD	11.4	-0.030	0.010
FS + SD + FR + FS:SD + FS:FR	12.8	-0.019	0.044
FR + FS + SD + FS:SD	12.9	-0.035	0.013
Peak Acceleration			
SD + FR + SD:FR	0.0	0.101	0.122
SD + FS + FR + SD:FS + SD:FR	1.9	0.114	0.162
FR + FS + SD + FR:FS + FR:SD	2.1	0.112	0.160
FS + SD + FR + SD:FR	2.2	0.099	0.133
FS + SD + FR + FS:SD + FS:FR + SD:FR	2.3	0.124	0.185
SD + FR	3.5	0.069	0.083
FS + SD + FR	5.8	0.067	0.095
FS + SD + FR + FS:SD + FS:FR + SD:FR + FS:SD:FR	6.2	0.110	0.185
SD + FS + FR + FS:FR	6.7	0.074	0.117
FR	6.8	0.038	0.045
FR + FS + SD + FS:SD	8.2	0.063	0.107
SD	9.4	0.019	0.026
FS + SD + FR + FS:SD + FS:FR 9.5 0.125 0.067	9.5	0.067	0.125
FS + FR	10.1	0.028	0.051
FS + FR + FS:FR	11.7	0.030	0.068
FS + SD	12.0	0.014	0.037
FS + SD + FS:SD	14.1	0.012	0.050
FS	14.1	-0.010	0.005

All combinations of the variables flow speed (FS), stimulus direction (SD), and the covariate of fineness ratio (FR) as well as all interactions were considered.

Interactions are represented by colons.

Table S2. Model selection analysis results for escape angle at the end of stage 1 of the escape response from (A) the original orientation of the fish and (B) from the stimulus position.

A Original orientation of the fish

Model	ΔAIC	Adjusted R^2	R^2
SD	0.0	0.157	0.169
SD + FR	1.5	0.153	0.173
FS + SD	3.5	0.147	0.173
SD + FR + SD:FR	4.7	0.145	0.177
FS + SD + FR	4.9	0.144	0.176
SD + FS + FR + FS:FR	5.3	0.153	0.198
FR + FS + SD + FR:FS + FR:SD	7.9	0.149	0.207
FS + SD + FR + SD:FR	8.1	0.135	0.181
FS + SD + FS:SD	9.8	0.130	0.183
FR + FS + SD + FS:SD	11.5	0.125	0.185
FS + SD + FR + FS:SD + FS:FR	12.4	0.131	0.203
SD + FS + FR + SD:FS + SD:FR	14.9	0.115	0.189
FS + SD + FR + FS:SD + FS:FR + SD:FR	15.0	0.126	0.212
FS + SD + FR + FS:SD + FS:FR + SD:FR + FS:SD:FR	17.4	0.133	0.244
FR	20.2	0.011	0.018
FS + FR	22.6	0.008	0.030
FS	23.5	-0.006	0.009
FS + FR + FS:FR	24.3	0.010	0.047

B Stimulus position

Model	ΔAIC	Adjusted R^2	R^2
SD	0.0	0.665	0.668
SD + FR	1.8	0.663	0.668
FS + SD	3.1	0.663	0.670
SD + FR + SD:FR	3.3	0.662	0.669
FS + SD + FR	4.8	0.661	0.670
SD + FS + FR + FS:FR	5.0	0.665	0.679
FS + SD + FR + SD:FR	6.2	0.660	0.672
FR + FS + SD + FR:FS + FR:SD	6.4	0.664	0.680
FS + SD + FS:SD	7.0	0.658	0.670
FR + FS + SD + FS:SD	8.7	0.656	0.671
FS + SD + FR + FS:SD + FS:FR	8.9	0.660	0.679
SD + FS + FR + SD:FS + SD:FR	10.0	0.655	0.672
FS + SD + FR + FS:SD + FS:FR + SD:FR	10.2	0.659	0.681
FS + SD + FR + FS:SD + FS:FR + SD:FR + FS:SD:FR	12.9	0.657	0.684
FR	156.8	-0.002	0.005
FS	157.2	0.002	0.016
FS + FR	158.5	0.000	0.021
FS + FR + FS:FR	159.5	0.006	0.041

Variable coding follows Table S1.

Table S3. Model selection analysis results for (A) response (if the fish exhibited an escape response when stimulated) (B) escape angle 30ms after escape response commencement (C) peak velocity and (D) peak acceleration.

A Response

Model	ΔAIC	Adjusted R^2	R^2
FS + SD + FS:SD	0.0	0.168	0.253
FR + FS + SD + FS:SD	1.9	0.159	0.254
FS + SD + FR + FS:SD + FS:FR	2.5	0.156	0.270
FS + SD + FR + FS:SD + FS:FR + SD:FR	4.8	0.145	0.278
SD + FS + FR + SD:FS + SD:FR	4.8	0.145	0.259
FS + SD + FR + FS:SD + FS:FR + SD:FR+ FS:SD:FR	5.8	0.141	0.311
SD + FS + FR + FS:FR	6.6	0.137	0.213
FS + SD	6.6	0.137	0.184
FS + SD + FR	8.4	0.128	0.185
FR + FS + SD + FR:FS + FR:SD	9.6	0.123	0.217
SD	10.2	0.120	0.148
FS + SD + FR + SD:FR	12.2	0.110	0.186
SD + FR	12.2	0.110	0.148
SD + FR + SD:FR	15.9	0.093	0.150
FS	33.7	0.008	0.037
FS + FR + FS:FR	34.6	0.004	0.061
FS + FR	35.6	0.000	0.037
FR	39.5	-0.019	0.000

B Escape angle at 30ms

Model	ΔAIC	Adjusted R^2	R^2
SD	0.0	0.110	0.124
SD + FR	1.6	0.106	0.126
SD + FR + SD:FR	3.3	0.108	0.141
SD + FS + FR + FS:FR	3.6	0.118	0.164
FS + SD	3.6	0.100	0.126
FR + FS + SD + FR:FS + FR:SD	4.3	0.126	0.184
FS + SD + FR	5.1	0.096	0.129
FS + SD + FR + SD:FR	7.1	0.095	0.142
FS + SD + FS:SD	8.6	0.091	0.145
FS + SD + FR + FS:SD + FS:FR	9.6	0.103	0.176
FR + FS + SD + FS:SD	10.3	0.086	0.147
FS + SD + FR + FS:SD + FS:FR + SD:FR	10.8	0.107	0.193
SD + FS + FR + SD:FS + SD:FR	12.8	0.081	0.156
FS + SD + FR + FS:SD + FS:FR + SD:FR + FS:SD:FR	13.0	0.115	0.227
FR	13.6	0.009	0.016
FS + FR	15.7	0.008	0.030
FS	16.1	-0.003	0.012
FS + FR + FS:FR	16.2	0.018	0.055

C Peak velocity

Model	ΔAIC	Adjusted R^2	R^2
SD + FR + SD:FR	0.0	0.026	0.062
FR	0.5	-0.006	0.002
FS	1.9	-0.009	0.006
FS + SD + FR + SD:FR	2.3	0.023	0.074
SD	2.5	-0.013	0.002
FR + FS + SD + FR:FS + FR:SD	3.3	0.030	0.094
FS + FR	3.6	-0.014	0.009
FS + FR + FS:FR	3.9	-0.002	0.035
SD + FR	4.3	-0.019	0.003
FS + SD + FR + FS:SD + FS:FR + SD:FR	4.7	0.045	0.137
SD + FS + FR + SD:FS + SD:FR	5.5	0.027	0.106

FS + SD	5.7	-0.023	0.007
FS + SD + FR	7.4	-0.028	0.010
SD + FS + FR + FS:FR	7.8	-0.017	0.035
FS + SD + FR + FS:SD + FS:FR	8.1	0.008	0.089
FS + SD + FS:SD	8.6	-0.016	0.044
FR + FS + SD + FS:SD	10.6	-0.024	0.044
FS + SD + FR + FS:SD + FS:FR + SD:FR + FS:SD:FR	11.0	0.025	0.148

D Peak acceleration

Model	ΔAIC	Adjusted R^2	R^2
SD + FR + SD:FR	0.0	0.066	0.100
SD + FR	0.9	0.047	0.068
FS + SD + FR + SD:FR	1.7	0.067	0.115
FR	1.8	0.026	0.034
SD + FS + FR + SD:FS + SD:FR	2.3	0.088	0.163
FS + SD + FR	3.7	0.040	0.075
FR + FS + SD + FR:FS + FR:SD	4.2	0.063	0.125
SD	4.7	0.012	0.027
FS + SD + FR + FS:SD + FS:FR + SD:FR	5.2	0.081	0.169
FS + FR	5.4	0.014	0.036
SD + FS + FR + FS:FR	5.6	0.040	0.090
FR + FS + SD + FS:SD	6.9	0.044	0.108
FS + SD	7.9	0.003	0.033
FS + FR + FS:FR	8.0	0.009	0.046
FS	8.1	-0.013	0.002
FS + SD + FR + FS:SD + FS:FR	8.4	0.046	0.124
FS + SD + FS:SD	9.2	0.021	0.079
FS + SD + FR + FS:SD + FS:FR + SD:FR + FS:SD:FR	12.3	0.056	0.175

Variable coding follows Table S1.

Table S4. Summary statistics of escape angle, fineness ratio, peak velocity, peak acceleration, and percent failure for each of the nine treatments

	Escape Angle (°)		Fineness Ratio		Velocity (cm/s)		Acceleration (cm/s^2)		Percent Failure	
Treatment	N	Mean±SE	N	Mean±SE	N	Mean±SE	N	Mean±SE	N	Percent
cr_00	15	54.69±9.41	17	7.90±0.12	15	73.35±8.46	15	8076.11±1039.05	19	11
cr_15	16	69.81±10.20	16	8.26±0.15	16	77.66±7.11	16	8724.68±1018.96	21	24
cr_30	5	69.10±9.11	6	7.54±0.15	6	68.84±14.60	6	9202.88±1241.33	20	70
la_00	12	43.51±11.83	16	8.27±0.16	12	82.45±8.33	12	9084.11±1098.53	21	24
la_15	15	37.32±7.63	16	8.23±0.12	15	62.83±5.73	15	6914.34±697.29	29	45
la_30	12	29.98±7.07	12	8.84±0.16	13	76.43±5.68	13	9082.76±744.59	16	25
ca_00	23	36.12±5.47	26	8.25±0.11	22	77.52±4.75	22	7225.89±607.54	27	4
ca_15	16	36.71±8.63	19	8.37±0.20	16	77.59±3.62	16	8008.38±586.07	20	5
ca_30	23	36.88±5.74	23	8.16±0.12	23	73.77±5.06	23	7255.49±535.37	23	0
Grand Mean	137	43.73±2.88	151	8.23±0.05	138	74.82±2.12	138	7976.33±268.02	197	23

N, number of fish tested for each treatment.

SE, standard error for each mean.

For evaluations of "percent failure," fish that did respond, but moved out of the frame before 30ms elapsed, were considered as successes in the total sample.

Treatment abbreviations follow the format of figure S1.